JACS
JOURNAL OF THE AMERICAN CHEMICAL SOCIETY

ARTICLE

pubs.acs.org/JACS

Hexameric Supramolecular Scaffold Orients Carbohydrates To Sense Bacteria

Dan Grünstein,[†] Maha Maglinao,[†] Raghavendra Kikkeri,[†] Mayeul Collot,[†] Konstantin Barylyuk,[‡] Bernd Lepenies,[†] Faustin Kamena,[†] Renato Zenobi,[‡] and Peter H. Seeberger*[,†]

[†]Department of Biomolecular Systems, Max Planck Institute of Colloids and Interfaces, Am Mühlenberg 1, 14476 Potsdam, Germany, and Institute of Chemistry and Biochemistry, Free University Berlin, Arnimallee 22, 14195 Berlin, Germany

[‡]Department of Chemistry and Applied Biosciences, ETH Zurich, Wolfgang-Pauli-Strasse 10, 8093 Zurich, Switzerland

Supporting Information

ABSTRACT: Carbohydrates are integral to biological signaling networks and cell−cell interactions, yet the detection of discrete carbohydrate−lectin interactions remains difficult since binding is generally weak. A strategy to overcome this problem is to create multivalent sensors, where the avidity rather than the affinity of the interaction is important. Here we describe the development of a series of multivalent sensors that self-assemble via hydrophobic supramolecular interactions. The multivalent sensors are comprised of a fluorescent ruthenium(II) core surrounded by a heptamannosylated β-cyclodextrin scaffold. Two additional series of complexes were synthesized as proof-of-principle for supramolecular self-assembly, the fluorescent core alone and the core plus β-cyclodextrin. Spectroscopic analyses confirmed that the three mannosylated sensors displayed 14, 28, and 42 sugar units, respectively. Each complex adopted original and unique spatial arrangements. The sensors were used to investigate the influence of carbohydrate spatial arrangement and clustering on the mechanistic and qualitative properties of lectin binding. Simple visualization of binding between a fluorescent, multivalent mannose complex and the *Escherichia coli* strain ORN178 that possesses mannose-specific receptor sites illustrates the potential for these complexes as biosensors.

INTRODUCTION

Carbohydrate−lectin interactions are critical to many biological systems.[1] Consequently, a better understanding of their interplay will provide important insights into specific biological processes. The weak affinities of carbohydrate−protein binding require improved tools to analyze carbohydrate−lectin complexes. Detection and read-out of binding can be improved by multivalent probes since they amplify the weak interactions and enhance the potency of carbohydrate ligands.

Many multivalent carbohydrate-based tools such as dendrimers,[2] polymers,[3] micelles,[4] and nanoparticles,[5] as well as carbohydrates built on templates of cyclodextrins (CDs)[6] and calixarenes,[7] have been synthesized to monitor glycan−lectin recognition and binding events by electronic, optical, or microgravimetric methods.[8] These multivalent probes can be functionalized with carbohydrates either through linear synthesis, where the sugar building blocks are incorporated during the synthetic process ("building-with-a-template"), or via convergent synthesis, where sugar functionalization takes place as a discrete, final step ("building-on-a-template").[3f,5a] "Building-on-a-template" is advantageous for generating libraries of multivalent carbohydrate-based probes, as different carbohydrate groups can be displayed by a variety of synthetic methods on a "fixed" core structure.

Important considerations for designing multivalent probes are valency, the spatial arrangement of the lectin target's multiple binding sites, and the response to external stimuli, such as biological or chemical triggering by carbohydrate−lectin binding.[9] No ideal scaffold for multivalent carbohydrate presentation exists, even though a myriad of systems have been described. For instance, C_5-symmetrical glycoconjugates that orient five ganglioside GM1 pentasaccharides can neutralize the pentameric cholera toxin via a specific, multivalent interaction.[10] Similarly, a multivalent C_3-symmetrical ganglioside GM3 trisaccharide is a potent inhibitor of influenza virus hemagglutination.[11]

With the goal of creating a new architecture for multivalent sugar presentation using the "building-on-a-template" strategy, we have developed a small-molecule scaffold that is synthetically facile and robust, has tunable symmetry, can accommodate different means of carbohydrate ligand functionalization, and exhibits distinct optical and electrochemical properties. This platform is based on hydrophobic supramolecular interactions that allow for the self-assembly of a fluorescent scaffold with a multivalent system, generating fluorescent and multivalent sensors. The fluorescent core—the template—is derived from $[Ru(bipy)_2]Cl_2$ to afford a di-adamantyl- (Ru2 **2**), tetra-adamantyl- (Ru4 **3**), or hexa-adamantyl-ruthenium(II) complex (Ru6 **4**). Around this core, β-cyclodextrins (βCD), each equipped with seven mannose units to form heptamannosylated βCD[12] (βCDMan), self-assemble around the template, as the adamantyl

Received: April 21, 2011
Published: July 26, 2011

Scheme 1. Overview of the Synthesis Procedure for the Ru Series 2−4

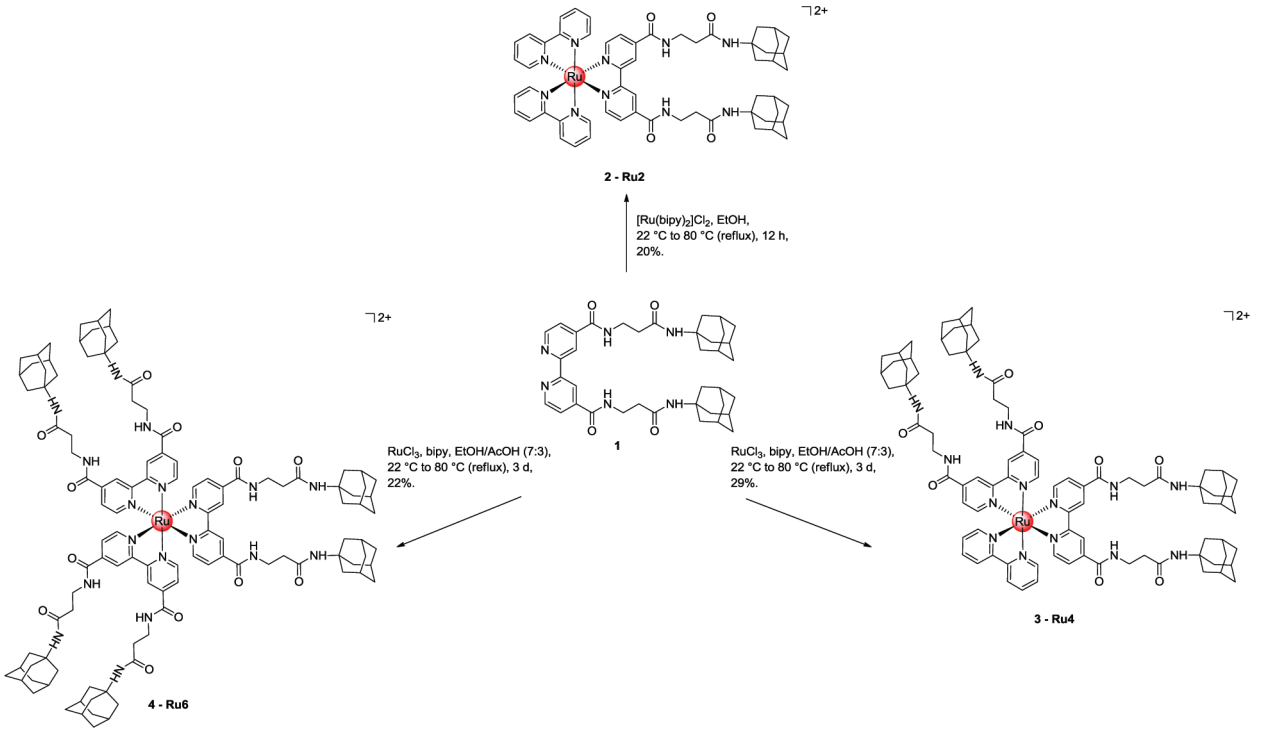

"hosts" the CD "guests" around the template. Two different series of fluorescent compounds were produced by the host−guest interactions. One group of molecules contains only unmodified βCD (RuCD2 **5**, RuCD4 **6**, and RuCD6 **7**). The second group of molecules consists of RuCDMan2 **8**, RuCDMan4 **9**, and RuCDMan6 **10**, bearing 14, 28, or 42 mannose units, respectively. Multivalent carbohydrate presentation and lectin binding were examined using the RuCDMan complexes **8**−**10** and the lectin concanavalin A (ConA). Surface plasmon resonance (SPR) measurements provided mechanistic, qualitative, and quantitative insights into the role of cluster arrangement. The fluorescence emission of the Ru(II) core was employed to visualize specific and shape-dependent interactions of **10** with *Escherichia coli* (*E. coli*) strain ORN178, which exhibits mannose-specific receptor sites for recognition and binding to host cells.

RESULTS AND DISCUSSION

Three variants of a fluorescent template were synthesized using common ligand **1** (Scheme 1) and produced three scaffolds with distinct architectures to support the multivalent presentation of carbohydrate ligands. Ligand **1** was obtained via a convergent synthesis (see Supporting Information (SI)). The scaffolds were comprised of a central ruthenium(II) core that is equipped with either two (Ru2 **2**), four (Ru4 **3**), or six (Ru6 **4**) adamantyl groups (Scheme 1). The di-adamantyl complex **2** was assembled by ligand complexation of **1** with $[Ru(bipy)_2]Cl_2$. Treatment of **1** with $RuCl_3$, using acetic acid as a reducing agent followed by bipyridine as a quenching agent, resulted in a mixture of tetra-adamantyl **3** and hexa-adamantyl **4** complexes, which were purified and separated by column chromatography.

To demonstrate the supramolecular interaction between CD derivatives and the adamantyl Ru(II) cores, complexes **2**−**4** were mixed with stoichiometric amounts (2, 4, and 6 equiv) of native βCD to furnish compounds with two (RuCD2 **5**), four (RuCD4 **6**), and six (RuCD6 **7**) CD units (Scheme 2).

Finally, a series of multivalent mannosylated structures was generated by mixing complexes **2**−**4** with βCDMan in water in stoichiometric amounts relative to the number of adamantyl units to afford RuCDMan2 **8**, RuCDMan4 **9**, and RuCDMan6 **10**. These multivalent complexes expose 14, 28, or 42 mannose units on their periphery, respectively (Scheme 3). It should be noted that complexes **2**−**4** can self-assemble with βCD carrying diverse glycosylation patterns, thereby facilitating production of a library of new multivalent systems.

Their octahedral core symmetry and robustness as well as strong oxidizing and reducing properties render ruthenium(II) complexes attractive for use as sensors.[13] The photophysical properties of the Ru series **2**−**4** were examined and compared with the properties of the RuCD series **5**−**7** to determine the effects of covering the ruthenium core with βCD (Figure 1a,b and Table 1). All spectra contain a first transition band (^{1}IL), located around 350 nm, that is assigned to metal-centered d−d transitions.[14] An intense absorption band at $\lambda_{max}^{abs} \approx 475$ nm and a shoulder at 450 nm dominate the spectra and originate from the splitting of the energy level of the first excited state caused by the trigonal symmetry of the complex. Both bands are assigned to a $t_{2g}(Ru) \rightarrow \pi^*(bipy)$ metal-to-ligand charge transfer (^{1}MLCT).[15] The emission spectra of the Ru series and the RuCD series exhibited an emission band at $\lambda_{max}^{em} \approx 640$ nm. An increase in emission intensity and calculated quantum yield (Φ) directly correlates with the increasing complexity of the structures as more units of ligand **1** and CD are assembled around the Ru(II) core (Figure 1c,d and Table 1).[16,17] Physical shielding of the core by

Scheme 2. Overview of the Synthesis Procedure for the RuCD Series 5−7

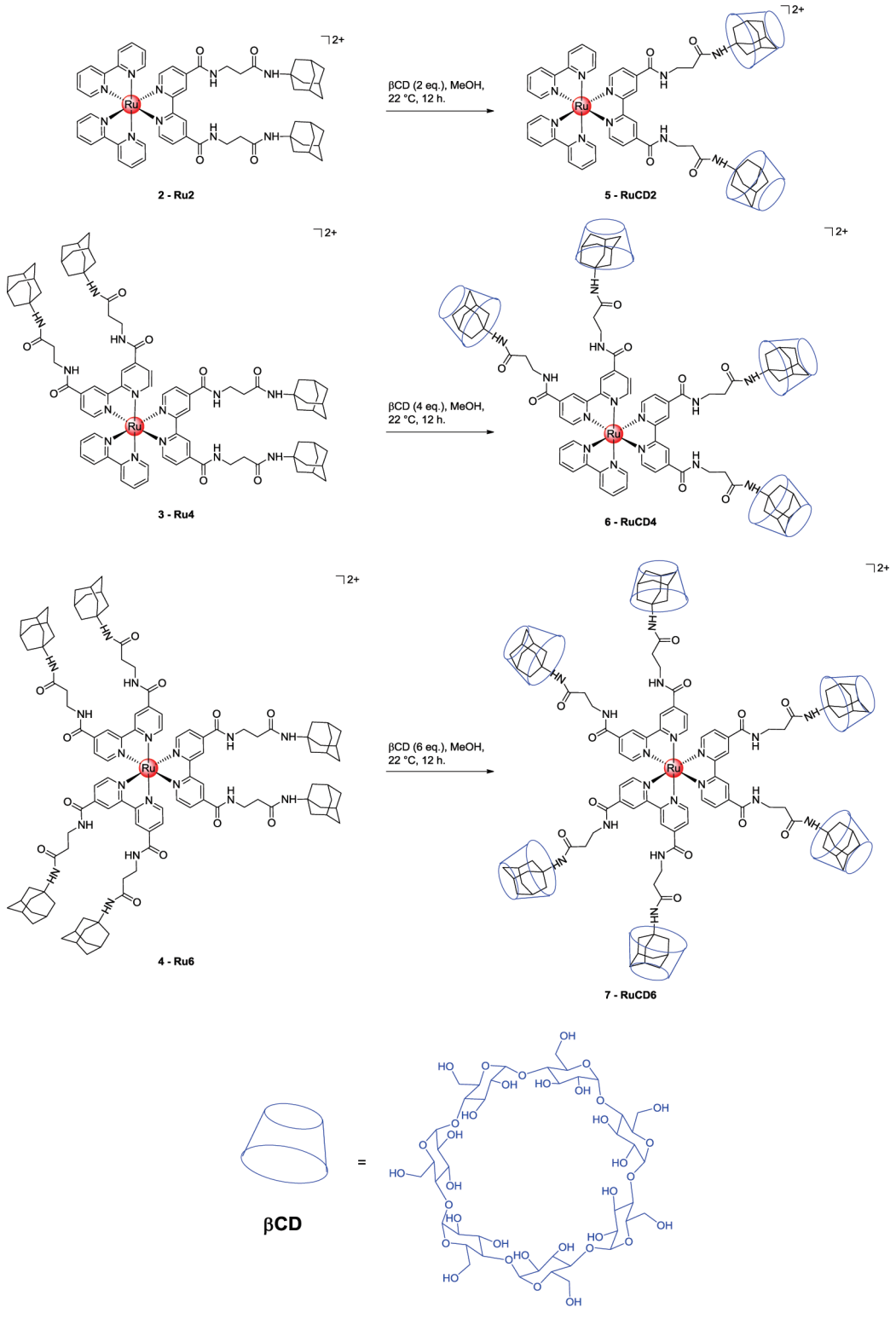

the surrounding scaffold prevents effective fluorescence quenching by dioxygen and solvent. Comparison of the quantum yields within the Ru series **2**−**4** illustrates the influence of the number of adamantyl ligands **1** on fluorescence intensity. The consequences of forming supramolecular assemblies, however, are highlighted by direct comparison of a Ru series complex and its RuCD equivalent, such as comparing **3** and **6**, or **4** and **7**. Interestingly, no difference was observed when **2** and **5** were compared. This is likely because complexes **2** and **5** differ by the addition of only two CDs, a minor structural difference, whereas an additional four CD molecules have been incorporated into complex **6**, and six CD molecules into complex **7**. While the bulky CDs in **6** and **7**

dx.doi.org/10.1021/ja2036767 |*J. Am. Chem. Soc.* 2011, 133, 13957–13966

Scheme 3. Overview of the Synthesis Procedure for the RuCDMan Series 8−10

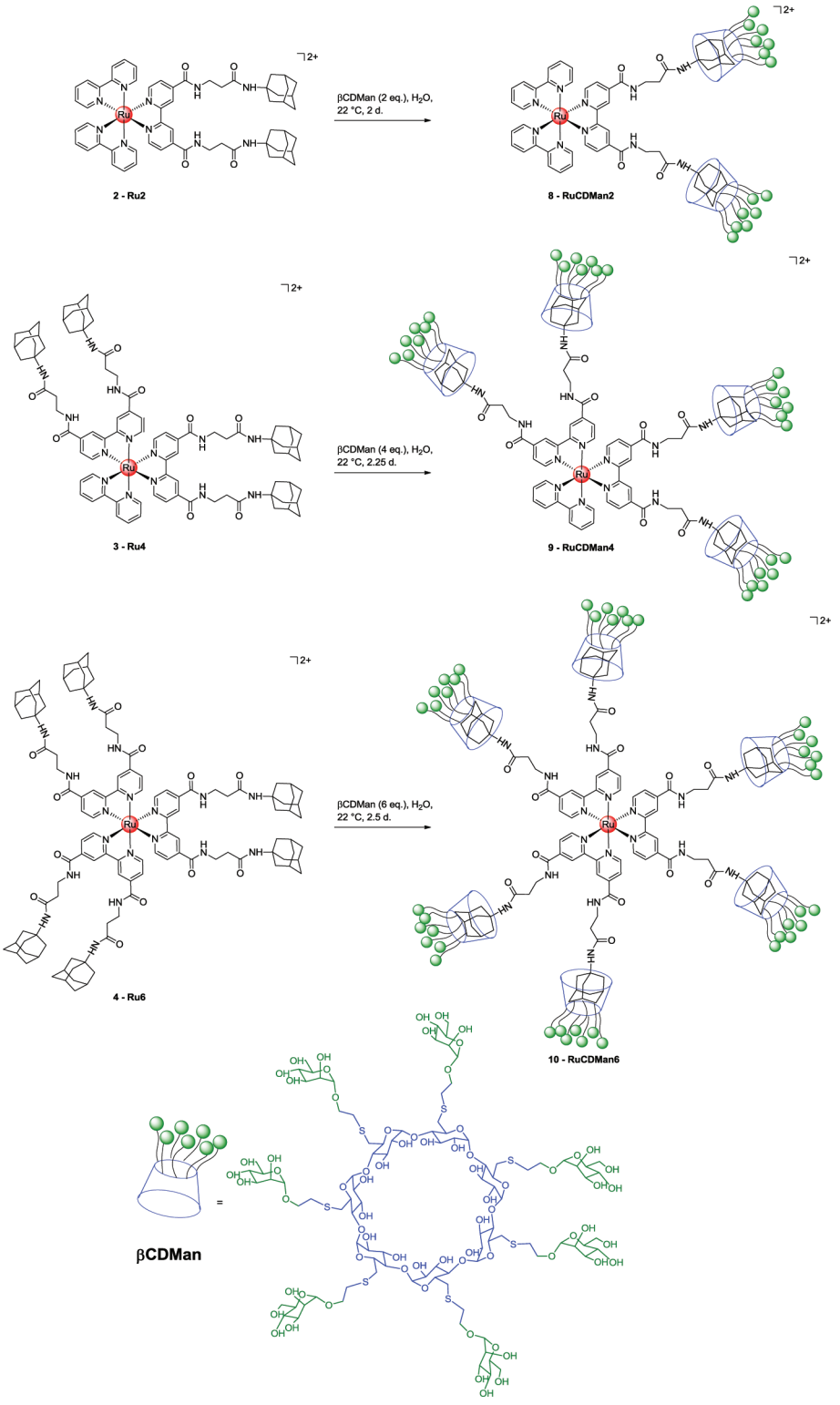

efficiently shield the fluorescent core from the environment, the two CDs in complex **5** are not sufficient, and consequently the fluorescent chromophore is easily quenched. Fluorescence peak analysis indicated a blue (hypsochromic) shift from 668.5 to 631.0 nm in the Ru series, and from 655.0 to 627.0 nm in the RuCD series, occurring as more adamantyl ligand **1** or more CD is added to the Ru(II) core. The observed hypsochromic shift of luminescence is possibly a consequence of so-called rigidochromism described in highly hindered complexes.[18] To summarize, an increasing number of adamantyl ligands **1** and, consequently, CD units around the metal center strongly influenced the photophysical and colloidal properties of the Ru(II) core.

dx.doi.org/10.1021/ja2036767 |*J. Am. Chem. Soc.* 2011, 133, 13957–13966

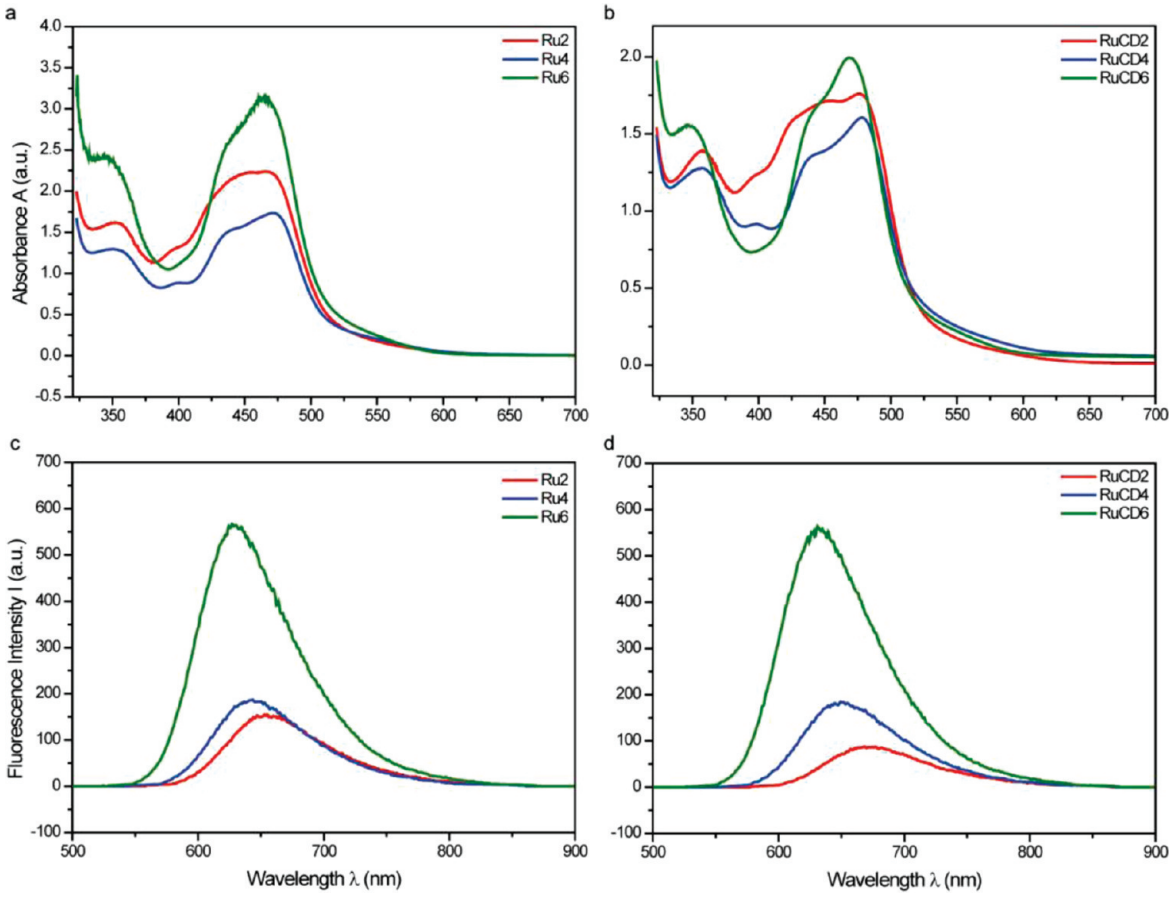

Figure 1. Absorption (UV) spectra of (a) the Ru series Ru2 **2**, Ru4 **3**, and Ru6 **4** in MeOH and (b) the RuCD series RuCD2 **5**, RuCD4 **6**, and RuCD6 **7** in H_2O. Emission (fluorescence) spectra of (c) the Ru series **2**−**4** in MeOH upon excitation at 475 nm and (d) the RuCD series **5**−**7** in H_2O upon excitation at 475 nm.

Table 1. Photophysical Data for Ruthenium Complexes 2−4 (in MeOH) and Complexes 5−7 (in H_2O)

complex	A_{max}	λ^{abs}_{max} (nm)	$\varepsilon_{\lambda^{abs}_{max}}$ ($L \cdot mol^{-1} \cdot cm^{-1}$)	λ^{em}_{max} (nm)	Φ
2	2.38	466.0	4760	668.5	0.14
3	1.73	471.0	3460	644.5	0.16
4	3.15	460.5	6300	631.0	0.48
5	1.76	477.0	5189	655.0	0.12
6	1.61	478.0	4586	641.5	0.23
7	1.99	468.5	5836	627.0	0.70

Encapsulation of the ruthenium(II) core with CD led to an increase in fluorescence intensity through protection of the core properties.

The RuCD complexes **5**−**7** were subjected to mass spectrometry to determine their stoichiometry and to analyze the supramolecular assemblies.[19,20] Only small amounts of the RuCDMan complexes **8**−**10** were available, and therefore these larger and heavier structures were not investigated. ESI is recognized as a soft ionization method that allows the generation of intact molecular ions from different species, including large, non-volatile organic molecules and biopolymers.[21] On the other hand, the detection of non-covalent assemblies by ESI-MS remains challenging since supramolecular interactions are often disrupted during the electrospray process. To keep non-covalent complexes intact during the ionization and ion transmission processes, a native nano-ESI technique was employed.[22]

Figure 2a shows the full scan of the RuCD2 **5** sample. The positive-ion mass spectrum of fully assembled complex **5** clearly reveals a doubly charged ion $[RuCD_2]^{2+}$ with m/z 1668. A broad isotope distribution due to the presence of Ru^{2+} is in agreement with the theoretically calculated isotope pattern (see Figures S3 and S4, SI). No Ru-containing ions with higher m/z values were detected in the mass spectrum, indicating the absence of non-specific aggregates of CD molecules and Ru-containing ligand either in the electrospray plume or inside the mass spectrometer.[19] Peaks at m/z 1100 and 533 corresponding to $[RuCD]^{2+}$ and $[Ru]^{2+}$ ions, respectively, were also detected. The presence of these ion peaks in the mass spectrum indicated partial dissociation of complex **5**. Acceleration and collision of the analyte ions with neutral gas molecules during the electrospray ionization process caused the observed dissociation of the supramolecular complex and could even lead to covalent bond cleavage under different conditions.[23]

The highlighted peaks in the full-scan mass spectrum of **6** (Figure 2b) correspond to ions from fully assembled $[RuCD_4]^{2+}$ (m/z 3050) and the partially assembled supramolecular complexes $[RuCD_3]^{2+}$ (m/z 2483), $[RuCD_2]^{2+}$ (m/z 1916), $[RuCD]^{2+}$ (m/z 1349), and $[Ru]^{2+}$ (m/z 781). No non-specific aggregates of Ru ligand and CD were evident in the higher m/z range.

dx.doi.org/10.1021/ja2036767 |J. Am. Chem. Soc. 2011, 133, 13957–13966

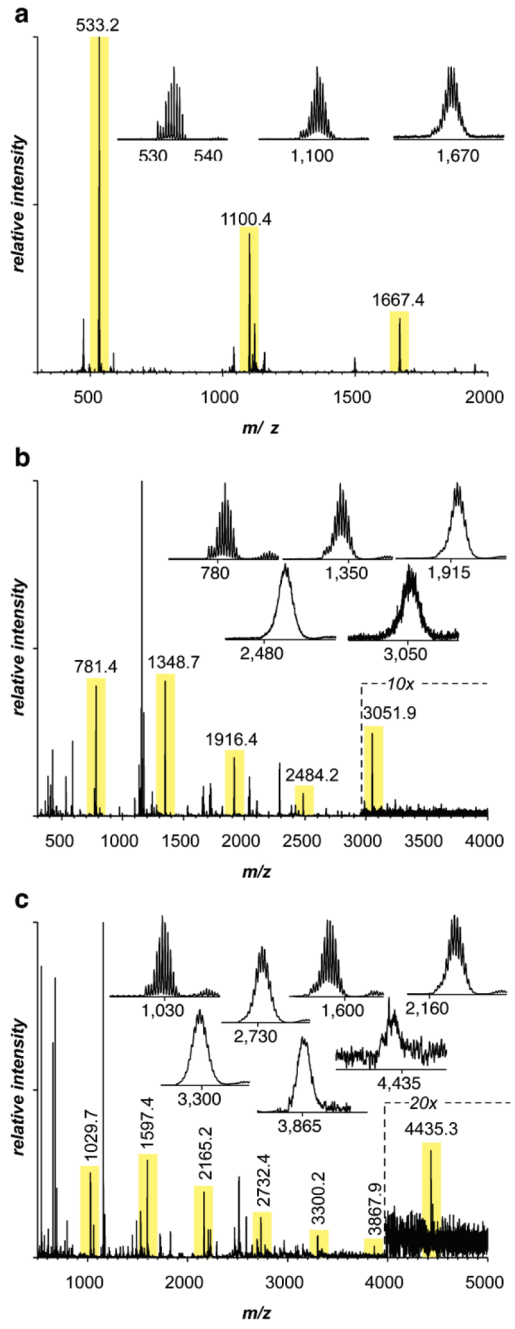

Figure 2. ESI mass spectra of (a) RuCD2 **5**, (b) RuCD4 **6**, and (c) RuCD6 **7**. Peaks corresponding to doubly charged ions of assembled, partially disassembled, and fully disassembled complexes are highlighted with yellow bars, marked with corresponding m/z values, and magnified (see insets).

Although a peak corresponding to the doubly charged ion of fully assembled RuCD4 complex **6** was detectable,[19] the resolution was not high enough to correctly resolve the individual isotope peaks (see Figures S5 and S6, SI).

A full-scan mass spectrum of RuCD6 **7** is shown in Figure 2c. Since the $[RuCD_6]^{2+}$ ion has a m/z value of ~4432, relatively high acceleration voltages were applied to the ion guides to facilitate ion transport. High acceleration of ions resulted in collision-activated dissociation of non-covalent complexes. Nevertheless, signals from ions of partially assembled RuCD6 complexes such as $[RuCD_5]^{2+}$ (m/z 3865), $[RuCD_4]^{2+}$ (m/z 3298), $[RuCD_3]^{2+}$ (m/z 2731), $[RuCD_2]^{2+}$ (m/z 2164), $[RuCD]^{2+}$ (m/z 1597), and $[Ru]^{2+}$ (m/z 1030) were detected in the mass spectrum (see Figures S7 and S8, SI). After the initial failure to measure the fully assembled complex **7** with conventional ESI and nano-ESI sources, different electrospray-based soft ionization methods, such as Electrosonic Spray Ionization (ESSI) and cold-spray, were employed. These measurements resulted in signals from $[RuCD_6]^{2+}$ above the detection limit and differences in ion yields for assembled, partially disassembled, and fully disassembled complexes were observed.[19]

Overall, nano-ESI mass spectrometry-based analysis of the RuCD complexes (**5**−**7**) confirmed the existence of complete supramolecular assembly. Stabilizing forces such as dispersion interactions between adamantyl moieties of the Ru(II)-containing ligands and the cavity of the CDs were insufficient to preserve the complexes from collision-activated dissociation, resulting in the presence of partially assembled complexes.

To confirm that the supramolecular assemblies are anchored by adamantyl groups acting as hosts in the CD guests, NMR was employed. Unfortunately, comparative measurements were complicated by the fact that some complexes (**2**−**4**) were soluble only in methanol, whereas others (**5**−**10**) were soluble only in water. ^{1}H NMR spectra were inconclusive in determining whether the inclusion complex between adamantyl moieties and native βCD or βCDMan occurred for each adamantyl group (see SI part 3.2). Different chemical shift patterns of the adamantyl protons were observed when comparing the ^{1}H NMR of different complexes and may have resulted from solvent effects rather than supramolecular assembly.

NOESY experiments[24] illustrated the proximity of the adamantyl groups to CD. Cross peaks arise from the proximity of the adamantyl moiety and CD via NOESY analysis of solutions of **5**, **6**, and **7** in D_2O (Figure 3a−c and Table 2). The cross peaks indicate strong interactions between H3 and H5 of βCD with all adamantyl protons (Ha, Hb, and Hc) throughout the RuCD complexes (Figure 4). Thus, it was confirmed that the adamantyl derivative penetrated completely into the βCD core. Since H2 and H4 of βCD are localized outside the cavity, they do not interact with adamantyl protons. All CD protons in the ^{1}H NMRs (complexes **5**−**7**) were shifted in comparison to the peaks of native βCD in D_2O, and proton signals signifying free native βCD were absent. All βCD units observed by NMR appear to be involved in supramolecular inclusion, indicating that all complexes were fully assembled.

Figure 3d−f shows the cross peaks observed from NOESY experiments for solutions of **8**, **9**, and **10** in D_2O. Due to the very complex ^{1}H NMR between 4.2 and 3.6 ppm, it was difficult to identify the H3 and H5 of βCDMan and assign changes after supramolecular assembly. Instead, we focused our attention on the protons of the adamantyl moiety and observed a strong NOE interaction with protons from the CDMan region. As described above for complexes **5**−**7**, three defined cross-coupling peaks appeared, coming from the interaction between CD and three different protons of the adamantyl moiety (Ha, Hb, and Hc). In comparison, for complexes **8**−**10**, the outermost protons of the adamantyl group (Hc) probably split due to the larger steric environment of βCDMan (attributable to the seven mannose residues).[25]

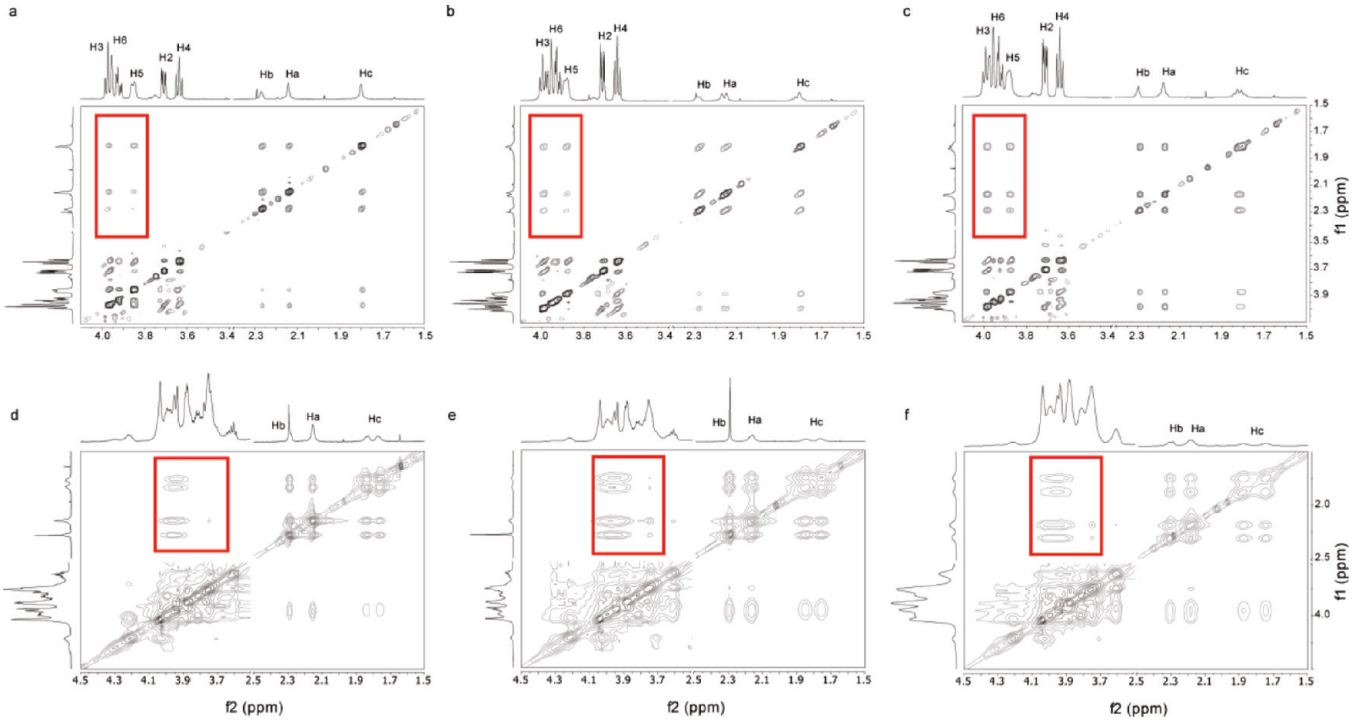

Figure 3. Significant cross peaks from the NOE spectra of (a) RuCD2 **5**, (b) RuCD4 **6**, and (c) RuCD6 **7** and of (d) RuCDMan2 **8**, (e) RuCDMan4 **9**, and (f) RuCDMan6 **10**. Cross peaks between H3 and H5 of βCD or βCDMan and Ha, Hb, and Hc of adamantyl are emphasized in the red boxes.

Table 2. ^{1}H NMR (in D_2O) Chemical Shifts of C−H Protons from Native βCD and from Ru(II)-Complexed βCD in the RuCD Series 5−7

	proton shift (ppm)					
entry	H1	H2	H3	H4	H5	H6
βCD	4.68	3.26	3.58	3.19	3.47	3.49
RuCD2 **5**	5.12	3.71	3.99−3.90	3.64	3.85	3.99−3.90
RuCD4 **6**	5.13	3.71	4.00	3.64	3.89	3.98−3.91
RuCD6 7	5.13	3.71	4.02−3.90	3.64	3.88	4.02−3.90

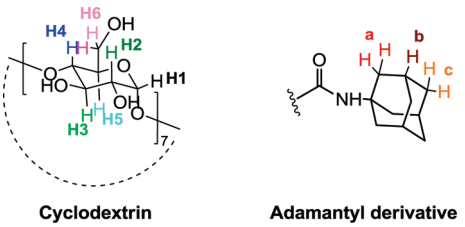

Figure 4. Proton designation of the relevant molecule moiety involved in the supramolecular assembly.

Overall, the results from the NOESY experiments clearly indicate that the inner βCD protons are in close proximity to the adamantyl moieties, confirming the presence of fully assembled complexes in the RuCD series **5**−**10**. Overall, the combination of photophysical and spectroscopic structural analyses provided a near-complete analytical characterization of complexes **2**−**10**. Functional studies were conducted to determine binding behavior of the multivalent RuCDMan complexes **8**−**10**.

Surface plasmon resonance (SPR) is a valuable tool for analyzing protein−carbohydrate complex formation in real time and for providing insights into the kinetics and mechanics of binding.[26] To understand the influence of mannose density on lectin binding at the surface of the RuCDMan complexes, the interaction of complexes **8**−**10** with the mannose-specific plant lectin ConA was investigated. SPR and kinetic analyses were based on a 1:1 interaction model.[27] Two different concentrations of ConA were covalently bound to a polycarboxylated CM5 sensor chip generating low-density (ConA-LD) and high-density (ConA-HD) surfaces. ConA has four mannose binding sites. Immobilizing the lectin at low and high densities was intended to distinguish whether the presence of more mannose-binding sites would stabilize bound complexes, or whether binding site clustering would inhibit this interaction.

The SPR analyses of ConA-RuCDMan2 **8** and ConA-RuCDMan4 **9** (Figure 5 and Table 3) indicated that both complexes **8** and **9** strongly prefer to bind ConA-HD over ConA-LD, indicating that high ConA concentration stabilized the binding interaction. This trend correlates well with the prior characterization of ConA binding to mannose.[28] Closer examination shows that **9** binds to ConA-HD more efficiently than **8**, and also that **8** dissociates from ConA much faster than **9** (Figure 5b,d). For the ConA-LD−complex interactions, K_D for **8** is lower than for **9**. The difference in the specific K_D values is most likely attributable to the generally weak binding of low ConA concentration than to the individual binding capacity of **8** and **9**. Interestingly, complex **10** did not bind to ConA (data not shown). The binding curves obtained for the interactions between **10** and ConA-HD as well as ConA-LD

dx.doi.org/10.1021/ja2036767 |J. Am. Chem. Soc. 2011, 133, 13957–13966

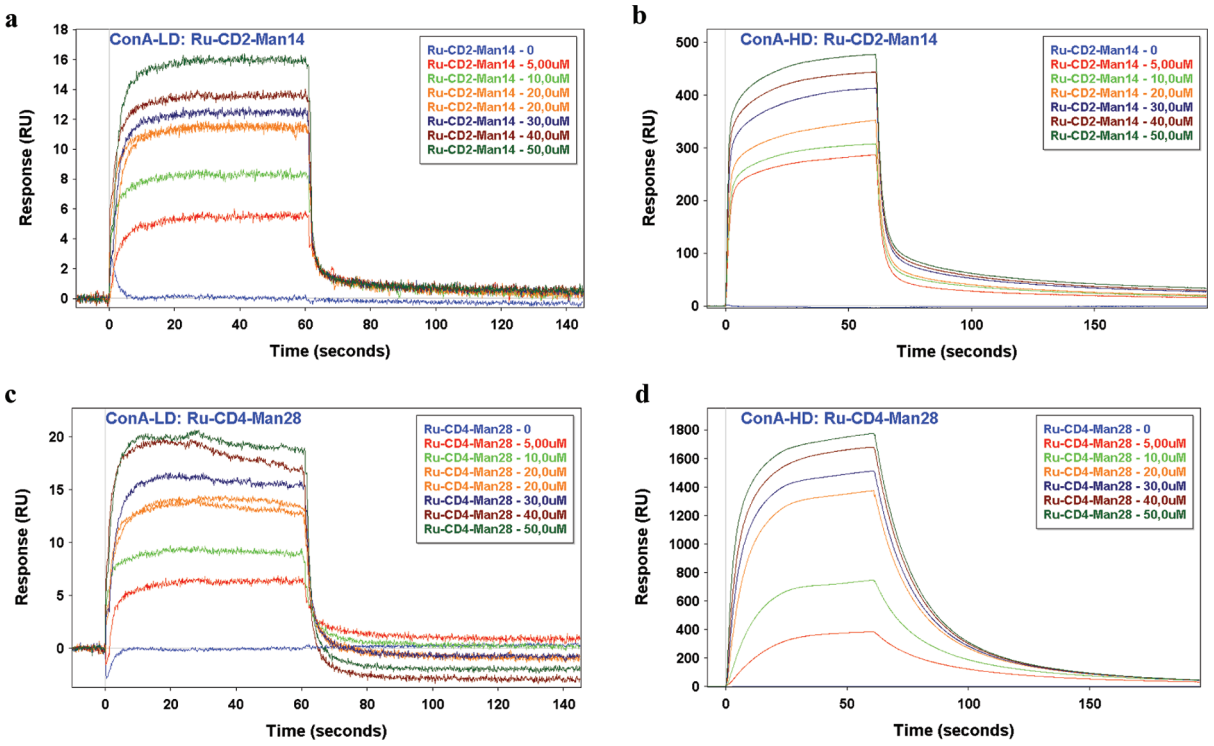

Figure 5. SPR sensorgrams of RuCDMan2 **8** (Ru-CD2-Man14) and RuCDMan4 **9** (Ru-CD4-Man28): (a,b) binding of RuCDMan2 **8** to ConA-LD and ConA-HD, respectively; (c,d) binding of RuCDMan4 **9** to ConA-LD and ConA-HD, respectively.

were comparable to the results obtained using only HEPES-EP as a negative control. This outcome is not entirely surprising, since similar results have been reported for highly multivalent probes.[29] In this case, the addition of two mannose-functionalized CD units (the structural difference between complexes **9** and **10**) impeded binding with ConA, despite the greater number of mannose residues available for the interaction. One explanation for this finding is that the inherent bulkiness of **10** may impede the formation of stable interactions between mannose and ConA. Additionally, the spatial arrangement of the mannose-bearing CDs is important: in the case of **10**, the mannose pattern may represent a non-ideal setup for interacting with surface-immobilized ConA. Together these results show that, in the context of a multivalent platform, the strength of the binding interaction between ConA and mannose directly correlates with the number of participating mannose residues. Nonetheless, there is an upper limit to that number, beyond which binding efficiency declines.

Since the binding capacity of complex **10** was unable to be assessed by SPR, an alternative strategy was devised using the outer surface of bacteria as the target for lectin recognition and binding. Two *E. coli* strains, ORN178 and ORN208, were used.[30] Both strains produce type 1 pili but differ in their expression of the pilus component *FimH*, a mannose-specific adhesin. While ORN178 expresses wild-type *FimH*, ORN208 carries a mutation in the fimH gene which renders the pili unable to bind mannose. Each bacterial strain was incubated with either complex **10** or the negative control, complex **7**, that does not contain mannose, and confocal microscopy was used to visualize the interaction between the complexes and the bacterial pili. The Ru(II)-containing complexes were observable by virtue of their inherent red fluorescence and the bacteria by using blue DAPI stain. Binding was evident only between mannosylated complex **10** and ORN178 (Figure 6a,b). Binding did not occur between complex **10** and strain ORN208 as anticipated due to the mutation in fimH[31] (Figure 6d). Other controls were performed to prove the specificity of the complex toward ORN178. As expected, complex **7** failed to bind to both ORN178 (Figure 6c) and ORN208 (Figure 6e).

Table 3. Equilibrium Constants, K_D, of RuCDMan2 8 and RuCDMan4 9

	K_D (μM)	
analyte	ConA-LD	ConA-HD
RuCDMan2 **8**	0.8428	0.2292
RuCDMan4 **9**	4.573	0.1380
RuCDMan6 **10**	no binding	no binding

The images obtained by confocal microscopy show red fluorescent spots (the Ru core) decorating the lateral end of the bacteria along the pili, implying that complex **10** is attached to the mannose-binding lectin *FimH* at this site. The molecular interaction between complex **10** and *E. coli* strain ORN178 was both specific and easily detectable, giving rise to the idea that this new fluorescent and highly multivalent system may be adapted to detect bacteria. Star-shaped clusters of bacteria were produced during incubation with **10** (Figure 6a,b) and may be attributable to the specific arrangement of this octahedral ruthenium complex. This will be the subject of future investigations.

dx.doi.org/10.1021/ja2036767 |*J. Am. Chem. Soc.* 2011, 133, 13957–13966

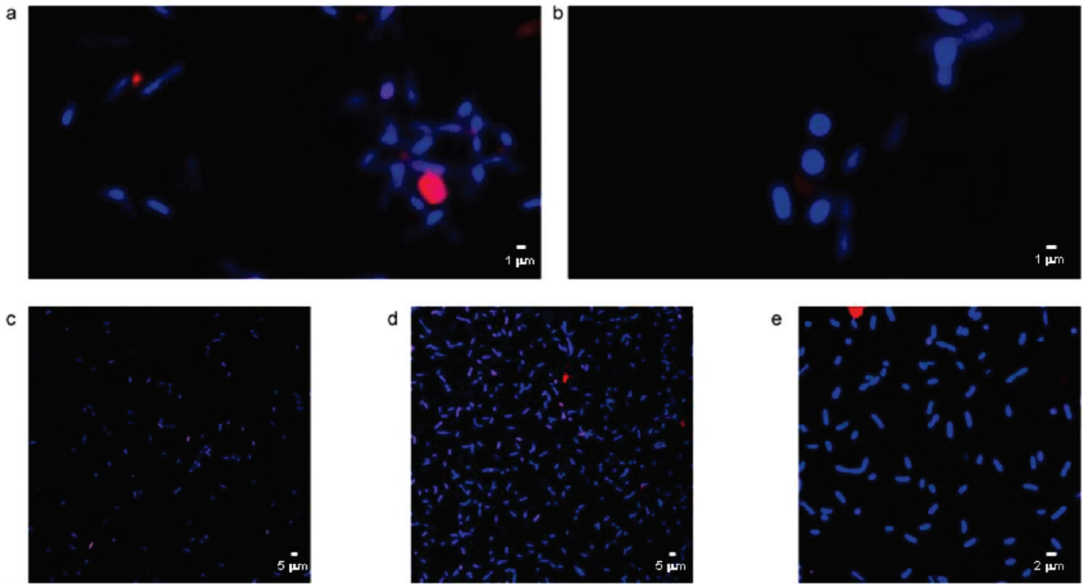

Figure 6. Confocal laser scanning microscopy images for the incubation of (a,b) bacteria *E. coli* strain ORN178 with RuCDMan6 **10** and of (c) ORN178 with RuCD6 **7**, (d) ORN208 with RuCDMan6 **10**, and (e) ORN208 with RuCD6 **7** as negative controls.

CONCLUSIONS

Here, we describe the synthesis of three different templates that ultimately generate three new scaffolds for the presentation of multiple multivalent carbohydrate ligands by supramolecular assembly. The multivalent complexes self-assemble and display carbohydrates with unique spatial orientation. In addition, binding interactions between the carbohydrate epitopes and lectins could be investigated by surface plasmon resonance. Previously, multivalent probes, such as supramolecular and conductive glycopolymers, carbohydrate-capped gold nanoparticles, and quantum dots, have been used as probes to identify specific *E. coli* strains[32] or other cell lines.[33] Taking advantage of the fluorescent properties of ruthenium(II), distinct interactions between mannosylated complex **10** and *E. coli* strain ORN178 were observed using confocal microscopy. The simplicity of this screen highlights the potential of using these complexes as adaptable and user-friendly bacterial sensing tools. The significance of another property of multivalent complexes was also illustrated by incubating complex **10** with ORN178: the bacterial clusters that formed around the complex were distinctive and star-shaped. Therefore, it is likely that the spatial arrangement of the ligands on the multivalent complex ultimately restricts the orientation of the lectins. Consequently, it may be possible to construct nanostructures that will interact with multiple target binding sites on bacterial cells or proteins in a shape-dependent manner, providing an easy visual read-out of a particular molecular interaction. Application of the multivalent probes to explore other carbohydrate−lectin interactions will be facilitated by the flexible architecture of this system—the mannosylated cyclodextrins are interchangeable with any glycosylated β-cyclodextrin. Simple interchange of the carbohydrate epitopes will also greatly streamline generating collections of multivalent probes.

ASSOCIATED CONTENT

Supporting Information. Details of syntheses, experiments, analyses and NMR spectra. This material is available free of charge via the Internet at http://pubs.acs.org.

AUTHOR INFORMATION

Corresponding Author
peter.seeberger@mpikg.mpg.de

ACKNOWLEDGMENT

P.H.S. and D.G. thank the Max-Planck Society and the European Union FP7 (CARMUSYS) for financial support. Generous financial support by the Körber Foundation is gratefully acknowledged. B.L. thanks the German Federal Ministry of Education and Research (BMBF, Fkz. 0315446) for financial support. The authors thank Dr. A. Schäfer for NMR spectroscopy and Dr. A. Springer for ESI-MS. We thank Dr. V. Mountain and Dr. R. Pragani for critically editing the manuscript.

REFERENCES

(1) (a) Drickamer, K.; Taylor, M. E. *Annu. Rev. Cell Biol.* **1993**, *9*, 237–264. (b) Liu, F. T. *Clin. Immunol.* **2000**, *97*, 79–88. (c) Konstantinov, K. N.; Robbins, B. A.; Liu, F. T. *Am. J. Pathol.* **1996**, *148*, 25–30. (d) Pilobello, K. T.; Slawek, D. E.; Mahal, L. K. *Proc. Natl. Acad. Sci. U.S.A.* **2007**, *104*, 11534–9. (e) Bertozzi, C. R.; Kiessling, L. L. *Science* **2001**, *291*, 2357–2364. (f) Lis, H.; Sharon, N. *Chem. Rev.* **1998**, *98*, 637–674.

(2) (a) Kikkeri, R.; Hossain, L. H.; Seeberger, P. H. *Chem. Commun.* **2008**, 2127. (b) De Paz, J. L.; Noti, C.; Boehm, F.; Werner, S.; Seeberger, P. H. *Chem. Biol.* **2007**, *14*, 879. (c) Wolfenden, E. K.; Cloninger, M. J. *J. Am. Chem. Soc.* **2005**, *127*, 12168. (d) Roy, R.; Kim, J. M. *Angew. Chem., Int. Ed.* **1998**, *38*, 369. (e) Woller, E. K.; Walter, E. D.; Morgan, J. R.; Singel, D. J.; Cloninger, M. J. *J. Am. Chem. Soc.* **2003**, *125*, 8820. (f) Kikkeri, R.; Liu, X. Y.; Adibekian, A.; Tsai, Y. H.; Seeberger, P. H. *Chem. Commun.* **2010**, *46*, 2197. (g) Lepenies, B.; Yin, J.; Seeberger, P. H. *Curr. Opin. Chem. Biol.* **2010**, *14*, 404. (h) Bernardes, G. J. L.; Kikkeri, R.; Maglinao, M.; Laurino, P.; Collot, M.; Hong, S. Y.; Lepenies, B.; Seeberger, P. H. *Org. Biomol. Chem.* **2010**, *8*, 4987.

(3) (a) Disney, M. D.; Zheng, J.; Swager, T. M.; Seeberger, P. H. *J. Am. Chem. Soc.* **2004**, *126*, 13343. (b) Yang, W.; Pan, C. Y.; Luo, M. D.; Zhang, H. B. *Biomacromolecules* **2010**, *11*, 1840. (c) Gestwicki, J. E.; Kiessling, L. L. *Nature* **2002**, *415*, 81. (d) Sasaki, K.; Nishida, Y.; Tsurumi,

T.; Uzawa, H.; Kondo, H.; Kobayashi, K. *Angew. Chem., Int. Ed.* **2002**, *41*, 4463. (e) Cario, C. W.; Gestwicki, J. E.; Kanai, M.; Kiessling, L. L. *J. Am. Chem. Soc.* **2002**, *124*, 1615. (f) Laurino, P.; Kikkeri, R.; Azzouz, N.; Seeberger, P. H. *Nano Lett.* **2011**, *11*, 73. (g) Gentsch, R.; Pippig, F.; Nilles, K.; Theato, P.; Kikkeri, R.; Maglinao, M.; Lepenies, B.; Seeberger, P. H.; Börner, H. G. *Macromolecules* **2010**, *43*, 9239–9247.

(4) Ryu, J. H.; Lee, E.; Lim, Y. B.; Lee, M. *J. Am. Chem. Soc.* **2007**, *129*, 4808–4814.

(5) (a) Kikkeri, R.; Laurino, P.; Odedra, A.; Seeberger, P. H. *Angew. Chem., Int. Ed.* **2010**, *49*, 2054. (b) Huang, C.-C.; Chen, C.-T.; Shiang, Y.-C.; Lin, Z.-H.; Chang, H.-T. *Anal. Chem.* **2009**, *81*, 875. (c) Lin, C.-C.; Yeh, Y.-C.; Yang, C.-Y.; Chen, C.-L.; Chen, G.-F.; Chen, C.-C.; Wu, Y.-C. *J. Am. Chem. Soc.* **2002**, *124*, 3508.

(6) (a) Gomez-Garcia, M.; Benito, J. M.; Rodriguez-Lucena, D.; Yu, J.-X.; Chmurski, K.; Mellet, C. O.; Gallego, R. G.; Maestre, A.; Defaye, J.; Fernandez, J. M. G. *J. Am. Chem. Soc.* **2005**, *127*, 7970. (b) Benito, J. M.; Gomez-Garcia, M.; Ortiz Mellet, C.; Baussanne, I.; Dafaye, J.; Fernandez, J. M.G. *J. Am. Chem. Soc.* **2004**, *126*, 10355. (c) Mellet, C. O.; Defaye, J.; Fernandez, J. M. G. *Chem.—Eur. J.* **2002**, *8*, 1982.

(7) (a) Fulton, D. A.; Stoddart, J. F. *Bioconjugate Chem.* **2001**, *12*, 655. (b) Baldini, L; Casnati, A.; Sansone, F.; Ungaro, R. *Chem. Soc. Rev.* **2007**, *36*, 254. (c) Badjic, J. D.; Nelson, A.; Cantrill, S. J.; Turnbull, W. B.; Stoddart, J. F. *Acc. Chem. Res.* **2005**, *38*, 723.

(8) (a) Kikkeri, R.; Kamena, F.; Gupta, T.; Hossain, L. H.; Boonyarattanakalin, S.; Gorodyska, G.; Beurer, E.; Coullerez, G.; Textor, M.; Seeberger, P. H. *Langmuir* **2010**, *26*, 1520. (b) Dai, Z.; Kawde, A.-N.; Xiang, Y.; La Belle, J. T.; Gerlach, J.; Bhavanandan, V. P.; Joshi, L.; Wang, J. *J. Am. Chem. Soc.* **2006**, *128*, 10018. (c) Kikkeri, R.; Grünstein, D.; Seeberger, P. H. *J. Am. Chem. Soc.* **2010**, *132*, 10230. (d) Otsuka, H.; Akiyama, Y.; Nagasaki, Y.; Kataoka, K. *J. Am. Chem. Soc.* **2001**, *123*, 8226. (e) Kikkeri, R.; Lepenies, B.; Adibekian, A.; Laurino, P.; Seeberger, P. H. *J. Am. Chem. Soc.* **2009**, *131*, 2110.

(9) Rosenzweig, B. A.; Ross, N. T.; Tagore, D. M.; Jayawickramarajah, J.; Saraogi, I.; Hamilton, A. D. *J. Am. Chem. Soc.* **2009**, *131*, 5020.

(10) (a) Fan, E. K.; Zhang, Z. S.; Minke, W. E.; Hou, Z.; Verlinde, C.; Hol, W. G. J. *J. Am. Chem. Soc.* **2000**, *122*, 2663. (b) Zhang, Z. S.; Merritt, E. A.; Ahn, M.; Roach, C.; Hou, Z.; Verlinde, C.; Hol, W. G. J.; Fan, E. *J. Am. Chem. Soc.* **2002**, *124*, 12991.

(11) Ohta, T.; Miura, N.; Fujitani, N.; Nakajima, F.; Niikura, K.; Sadamoto, R.; Guo, C. T.; Suzuki, T.; Suzuki, Y.; Monde, K.; Nishimura, S. I. *Angew. Chem., Int. Ed.* **2003**, *42*, 5186.

(12) Garcia-Barrientos, A.; Garcia-Lopez, J. J.; Isac-Garcia, J.; Ortega-Caballero, F.; Uriel, C.; Vargas-Berenguel, A.; Santoyo-Gonzalez, F. *Synthesis* **2001**, 1057.

(13) Kikkeri, R.; Garcia-Rubio, I.; Seeberger, P. H. *Chem. Commun.* **2009**, 235.

(14) Hahn, U.; Vogtle, F.; De Paoli, G.; Staffilani, M.; De Cola, L. *Eur. J. Inorg. Chem.* **2009**, 2639.

(15) Issberner, J.; Vogtle, F.; De Cola, L.; Balzani, V. *Chem.—Eur. J.* **1997**, *3*, 706.

(16) Faiz, J. A.; Kyllonen, L. E. P.; Contreras-Carballada, P.; Williams, R. M.; De Cola, L.; Pikramenou, Z. *Dalton Trans.* **2009**, 3980.

(17) Felici, M.; Contreras-Carballada, P.; Vida, Y.; Smits, J. M. M.; Nolte, R. J. M.; De Cola, L.; Williams, R. M.; Feiters, M. C. *Chem.—Eur. J.* **2009**, *15*, 13124.

(18) (a) Wrighton, M.; Morse, D. L. *J. Am. Chem. Soc.* **1974**, *96*, 998. (b) Innocenzi, P.; Kozuka, H.; Yoko, T. *J. Phys. Chem. B* **1997**, *101*, 2285.

(19) Barylyuk, K.; Balabin, R. M.; Grünstein, D.; Kikkeri, R.; Frankevich, V.; Seeberger, P. H.; Zenobi, R. *J. Am. Soc. Mass Spectrom.* **2011**, *22*, 1167.

(20) Hernandez, H.; Robinson, C. V. *Nat. Protoc.* **2007**, *2*, 715.

(21) (a) Fenn, J. B.; Mann, M.; Meng, C. K.; Wong, S. F.; Whitehouse, C. M. *Science* **1989**, *246*, 64. (b) Kebarle, P.; Verkerk, U. H. *Mass Spectrom. Rev.* **2009**, *28*, 898.

(22) Wilm, M.; Mann, M. *Anal. Chem.* **1996**, *68*, 1.

(23) Gabelica, V.; De Pauw, E. *Mass Spectrom. Rev.* **2005**, *24*, 566.

(24) Schneider, H. J.; Hacket, F.; Rudiger, V.; Ikeda, H. *Chem. Rev.* **1998**, *98*, 1755.

(25) Jing, B.; Chen, X.; Zhao, Y. R.; Wang, X. D.; Cai, J. G.; Qiu, H. Y. *J. Phys. Chem. B* **2008**, *112*, 7191.

(26) Rich, R. L.; Myszka, D. G. *J. Mol. Recognit.* **2006**, *19*, 478.

(27) Hardman, K. D.; Ainswort., C. F. *Biochemistry* **1972**, *11*, 4910.

(28) Munoz, E. M.; Correa, J.; Fernandez-Megia, E.; Riguera, R. *J. Am. Chem. Soc.* **2009**, *131*, 17765.

(29) (a) Dhayal, M.; Ratner, D. A. *Langmuir* **2009**, *25*, 2181. (b) Schlick, K. H.; Cloninger, M. J. *Tetrahedron* **2010**, *66*, 5305.

(30) Kim, B. S.; Hong, D. J.; Bae, J.; Lee, M. *J. Am. Chem. Soc.* **2005**, *127*, 16333.

(31) (a) Jones, C. H.; Pinkner, J. S.; Roth, R.; Heuser, J.; Nicholes, A. V.; Abraham, S. N.; Hultgren, S. J. *Proc. Natl. Acad. Sci. U.S.A.* **1995**, *92*, 2081. (b) Choudhury, D.; Thompson, A.; Stojanoff, V.; Langermann, S.; Pinker, J.; Hultgren, S. J.; Knight, S. D. *Science* **1999**, *285*, 1061. (c) Harris, S. L.; Spears, P. A.; Havell, E. A.; Hamrick, T. S.; Horton, J. R.; Orndorff, P. E. *J. Bacteriol.* **2001**, *183*, 4099.

(32) (a) Hahan, M. A.; Tabb, J. S.; Krauss, T. D. *Anal. Chem.* **2005**, *77*, 4861. (b) Mukhopadhyay, B.; Martins, M. B.; Karamanska, R.; Russell, D. A.; Field, R. A. *Tetrahedron Lett.* **2009**, *50*, 886. (c) Wang, C.; Irudayaraj, J. *Small* **2008**, *4*, 2204. (d) Huang, P. J.; Tay, L. L.; Tanha, J.; Ryan, S.; Chau, L. K. *Chem.—Eur. J.* **2009**, *15*, 9330. (e) Su, Y. L.; Li, J. R.; Jiang, L.; Cao, J. *J. Colloid Interface Sci.* **2005**, *284*, 114. (f) Li, Y.; Ma, B.; Fan, Y.; Kong, X.; Li, J. *Anal. Chem.* **2002**, *74*, 6349.

(33) Gottschaldt, M.; Schubert, U. S.; Rau, S.; Yano, S.; Vos, J. G.; Kroll, T.; Clement, J.; Hilger, I. *Chembiochem* **2010**, *11*, 649.